ELSEVIER

Journal of Power Sources 103 (2001) 72–79

JOURNAL OF POWER SOURCES

www.elsevier.com/locate/jpowsour

Photo-electrochemical characteristics of a cobalt–air cell using an anode active material–semiconductor (Co–GaP) hybrid electrode

Keiji Akuto*, Masaya Takahashi, Yoji Sakurai

NTT Telecommunications Energy Laboratories, Tokai, Ibaraki 319-1193, Japan

Received 27 October 2000; received in revised form 23 May 2001; accepted 5 June 2001

Abstract

An anode active material–semiconductor hybrid electrode was prepared by combining electroplated Co and a GaP single crystal. This hybrid electrode acts not only as an active material for a cobalt–air cell but also as a photo-electrode for storing light energy. We studied the photo-electrochemical properties of the hybrid electrode, and confirmed that the electrode's oxidized Co layer was reduced by the electrons generated when the GaP side was illuminated. We assembled a GaP–Co|KOH|O_2 cell with only two electrodes: the above hybrid electrode and an air electrode (oxygen catalyst). The photo-electrochemical characteristics of the Co–GaP hybrid electrode and cobalt–air cell showed that this cell can be charged by illuminating it and discharged by using the oxygen in the air.

Keywords: Active material–semiconductor hybrid electrode; Metal–semiconductor electrode; Cobalt–air cell; Photo-electrochemistry; Photo-charging

1. Introduction

Silicon solar cells using p–n junctions are often used with storage cells, such as lead–acid batteries or nickel–cadmium batteries, because the intensity of solar energy is not stable and its power density is low. In this case, light energy is converted to electrical energy, which is then converted to chemical energy. However, some energy is lost in each conversion. Moreover, the electrical power generated by the silicon solar cell must be regulated at a voltage and current suitable for charging the storage cell. Then, the control apparatus result in drop of the photo-charging efficiency and increase in total system size. Photo-electrochemical solar cells are an excellent alternative energy source, which can replace fossil fuels and maintain a clean environment [1–8]. In contrast, a photo-electrochemical rechargeable battery converts light energy to chemical energy directly, giving excellent potential for high efficiency. Furthermore, there have been several experimental attempts to store light energy electrochemically. These attempts led to the invention of photo-electrochemical rechargeable batteries [9–21]. For example, studies have been undertaken on the electrochemical characteristics of a GaP|$K_3[Fe(CN)_6]$–$K_4[Fe(CN)_6]$||-Ni^{2+}|Pt battery [9], a CdTe|$CdSO_4$|CdSe battery with an auxiliary bias provided by a Si p–n solar cell [10] and a photo-rechargeable battery with a layer compound $CuFeTe_2$ [19], and their fundamental feasibility was reported. These batteries contain electrolyte like conventional chemical storage cells and an electrode used for storing electricity.

In contrast, metal–air cells have an intrinsically high capacity because the cathode active material, oxygen in the air, is provided from outside the cell, implying that only the anode active material has to be contained in the cell [22]. We, therefore, anticipate that the discharge capacity of photo-electrochemical rechargeable batteries will be improved by combining them with metal–air cells. Previously developed photo-electrochemical rechargeable batteries incorporated three or four electrodes [20]. Such structures make the batteries more complex and reduce their energy density. Moreover, by attaching an insoluble active material to the back of a semiconductor electrode, we can construct an electrode that acts as both a photo-electrode and an active material. This means that we are able to assemble a photo-electrochemical rechargeable battery with a two-electrode construction using an electrode formed by combining an anode active material with a photo-electrode.

2. Concept of photo-electrochemical rechargeable battery

Our aim was to produce a photo-rechargeable cobalt–air cell by using an anode active material (Co)–semiconductor hybrid electrode and an oxygen catalyst as negative and

* Corresponding author. Fax: +81-29-287-7863.
E-mail address: akuto@iba.iecl.ntt.co.jp (K. Akuto).

0378-7753/01/$ – see front matter
PII: S0378-7753(01)00834-5

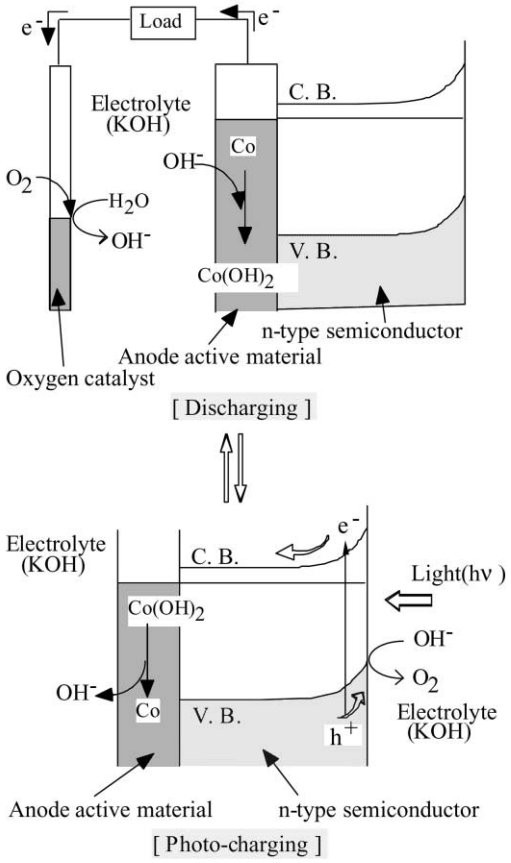

Fig. 1. Idealized energy-level diagram and reaction mechanism of photo-electrochemical rechargeable battery.

positive electrodes, respectively. This cell can be discharged by using the Co and the oxygen in the air as shown in Fig. 1. During discharge, the Co in the hybrid electrode is oxidized and the electrons are transferred to the positive electrode. They are drawn through the external circuit to the oxygen catalyst where reduction of the oxygen occurs. This discharge reaction then generates electric energy.

ZThe Co is converted into $Co(OH)_2$ during the discharge process. Our main reason for developing the hybrid electrode was to enable us to use it to store light energy as the reduction product of $Co(OH)_2$. Fig. 1 shows the idealized schematic energy level diagram and the reaction mechanism that we expect in the illuminated anode active material (Co)–semiconductor hybrid electrode. During light irradiation, the photoinduced electron–hole pairs are separated by an electrical field in the space–charge region of the semiconductor. The holes migrate towards the semiconductor/electrolyte interface and are consumed by the electrolyte for oxygen evolution. The electrons excited into the conduction band are transferred to the anode active material. As a result, the electrons reduce the $Co(OH)_2$ to Co, thus, achieving photo-reduction. This reaction on the hybrid electrode during illumination is just reverse of the above discharge reaction.

The output voltage of this cell is determined by the difference between the oxidation potential of the Co in the hybrid electrode and the reduction potential of the oxygen in the air electrode. To enable electron transfer from the conduction band edge of the semiconductor to the anode active material that is attached to the back of the semiconductor, we must choose a semiconductor and metal combination, which can make the situation that the flatband potential of the semiconductor is higher than the redox potential of the anode active material.

To meet this requirement, we selected an n-type GaP semiconductor for the hybrid electrode. We fabricated a Co–GaP hybrid electrode that works both as a photo-electrode and as an anode active material and examined its photo-electrochemical characteristics. During illumination, we expect the active material to be reduced by photoinduced electrons and the electrolyte to be oxidized by photoinduced holes. It is already known that the GaP dissolution reaction can be written as follows [23,24]:

$$GaP + 4OH^- + 3h^+ \rightarrow GaO_2^- + P + 2H_2O \quad (1)$$

Moreover, it has been reported that it is possible to stabilize a semiconductor electrode by modifying its surface with metal [25–27]. We predict a similar GaP dissolution in our hybrid electrode, but we used a GaP semiconductor and a Co metal to confirm the photo-charging capability because they have an optimum photoinduced energy level (flat band potential) (see Fig. 2, [28,29]). We have also assembled a two-electrode GaP–Co|KOH|O_2 cell by using this hybrid electrode and an air electrode and investigated its photo-charging behavior.

3. Experimental

3.1. Anode active material–semiconductor hybrid electrode fabrication

We fabricated anode active material–semiconductor hybrid electrodes by depositing metal films on a single-crystal

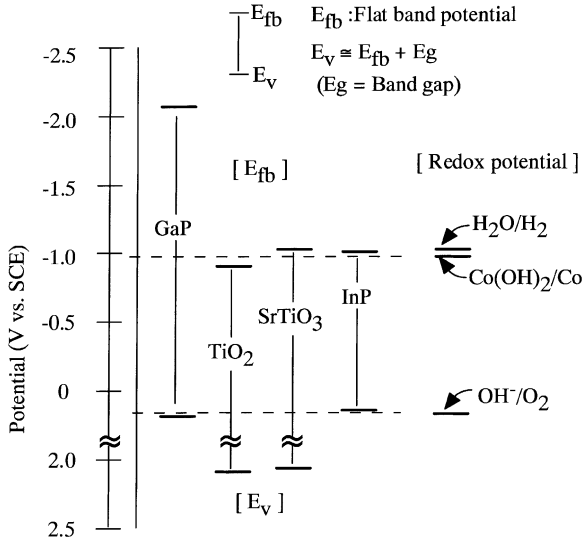

Fig. 2. Flat band potentials of n-type semiconductor (pH = 13–14).

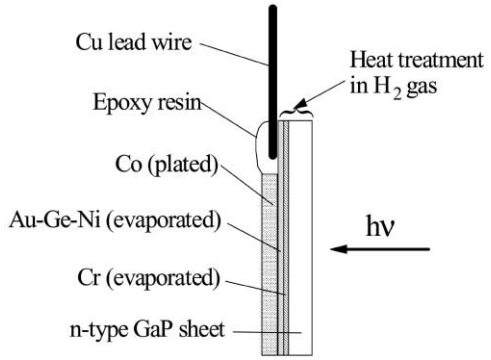

Fig. 3. Schematic diagram of the anode active material–semiconductor (Co–GaP) hybrid electrode.

semiconductor sheet. Fig. 3 is a schematic diagram of the hybrid electrode we used in this investigation. This electrode consists of Co metal as an anode active material and GaP semiconductor as a photo-absorption material (photo-electrode). We formed the Au–Ge–Ni and Cr layers between these two materials to make Ohmic junction, as described later.

Single-crystal n-type GaP wafers (Te doped), obtained from Sumitomo Metal Mining, were used as the semiconductor material. The crystals were oriented in the (1 1 1) direction. The GaP wafers were cut into sheets, each with a 2.2 cm^2 surface area on one side. We washed these sheets ultrasonically with a semiconductor cleaning solution (Semico Clean 23, Furuuchi Chemical), and then rinsed them ultrasonically with distilled and deionized water. Cr and Au–Ge–Ni alloy were evaporated on one side of the sheets using a surface preparator (PEC-A2, Shimazu) for evaporation. The Cr and Au–Ge–Ni layers were about 400 and 2500 Å thick, respectively. The evaporated layers were then annealed for 5 min at 600°C in a hydrogen atmosphere with an infrared lamp furnace (VHC-P610CP/7085, Shinku-Riko).

Next, a copper lead wire was soldered to the evaporated metal layer and the soldering point was covered with epoxy resin (Araldite, Chiba-Geigy). The Au–Ge–Ni evaporated side of GaP sheet was then electroplated with Co. The other side and edge, with the exposed GaP, were covered with a photoresist (TSMR-V3, Tokyo Ohka) to prevent Co from plating the GaP surface. The electroplating solution consisted of 0.89 M (mol dm^{-3}) cobalt sulfate, 0.21 M cobalt chloride, and 0.65 M boric acid. A voltage of 5 V was applied for 5 min between the GaP sheet and a graphite rod counter electrode, by using a bipolar power supply (POW 35-1A, Kikusui Electronics). The current density was about 400 mA cm^{-2}. During the electroplating, the solution was stirred and kept at 50°C. After the plating, the photoresist cover on the GaP surface was removed with use of 1 M KOH solution. We confirmed that removing the photoresist did not destroy the Co layer in the electrode. Hereafter, this electrode is denoted as a Co–GaP hybrid electrode.

We also fabricated a GaP (non-hybrid) electrode to measure the photo-electrochemical characteristics of the GaP itself. Its structure was the same as that of the Co–GaP hybrid electrode, except that it had no Co plating layer and the Au–Ge–Ni surface of the electrode was covered with epoxy resin.

3.2. Apparatus and procedure

The GaP–Co|KOH|O_2 cell we assembled consisted of a Co–GaP hybrid electrode and an air electrode. A schematic diagram of the cell assembly is shown in Fig. 4. A rectangular platinum mesh was used as the air electrode (oxygen catalyst). This mesh was placed parallel to and in contact with the electrolyte surface to ensure oxygen-reduction discharging by increasing the gas–liquid–solid three-phase boundary area. A quartz cylinder, 7 cm in diameter and 12 cm high, was used as the cell compartment, and 2 mol dm^{-3} potassium hydroxide solution was used as the electrolyte.

A 500 W Xe lamp (UI-501C, Ushio) was used as the illuminating light source. Its intensity was adjusted with an iris. The intensity was set at about 100 mW cm^{-2}, except during the reduced-intensity light source experiments.

The photo-charge characteristics of the cell were measured with a charge–discharge unit (HJ-201B, Hokuto Denko) and recorded on a graphic plotter (7550A, Hewlett-Packard). A Pyrex glass compartment contained an SCE reference electrode and the same kind of electrolyte as the cell. To monitor the GaP–Co hybrid electrode potential variation, this was connected to the cell with a Luggin capillary during cell charging and discharging. The potential was measured with a potentiostat (HA-501, Hokuto Denko) used as a potentiometer, and the results were recorded with a Y-T recorder (3056, Yokogawa Electric Works). The cyclic voltammograms of the GaP and Co–GaP electrode were measured with a potentiostat (HA-501G, Hokuto Denko) and an arbitrary function generator (HB-105, Hokuto Denko) coupled to a computer (PC-9801, NEC); and the

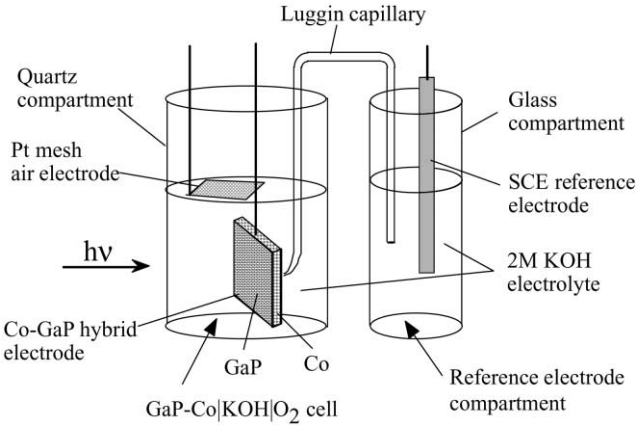

Fig. 4. Schematic diagram of experimental cell (GaP–Co|KOH|O_2) assembly.

results were recorded on the 7550A graphic plotter using a scan rate of 20 mV s^{-1}. The platinum mesh electrode and the SCE electrode were used as the auxiliary electrode and the reference electrode, respectively. All experiments were carried out at 25°C.

The discharged anode sample was characterized by X-ray diffraction (XRD) with Cu Kα radiation (Rigaku Rotaflex, Rint2000). We undertook elemental analyzes of the GaP/Au–Ge–Ni interface with a SIMS instrument (IMS-3F, CAMECA). The incident O_2^+ primary ion beam energy was 10.5 keV with a current of 0.5 μA. The diameter of the secondary ion analysis area was 60 μm.

4. Results and discussion

In the cobalt–air cell (Co|KOH|O_2), the Co anode is converted into $Co(OH)_2$ during the discharge process. This $Co(OH)_2$ was identified by XRD, as shown in Fig. 5. Fig. 5(a) shows the XRD pattern of anode electrode in the Co|KOH|O_2 cell after 30 min discharging at 0.5 mA cm^{-2}. The XRD pattern (b) was obtained in the Co electrode before discharging. The XRD peaks of the discharged sample indicated the $Co(OH)_2$ formation distinctly. This result is supported by the potential–pH equilibrium diagram for the system cobalt–water [30]. We attempted to fabricate a Co–GaP electrode to realize a photo-reducible anode for the cobalt–air cell. It is known that an energy barrier appears at most metal/semiconductor interfaces. To fabricate this anode active material–semiconductor hybrid electrode, Cr and Au–Ge–Ni alloy were evaporated on one side of GaP sheets to make Co–GaP Ohmic junction [31]. Au reduces the melting point of this alloy by forming eutectic crystals with Ge. The Au–Ge attracts Ga atoms, and encourages the

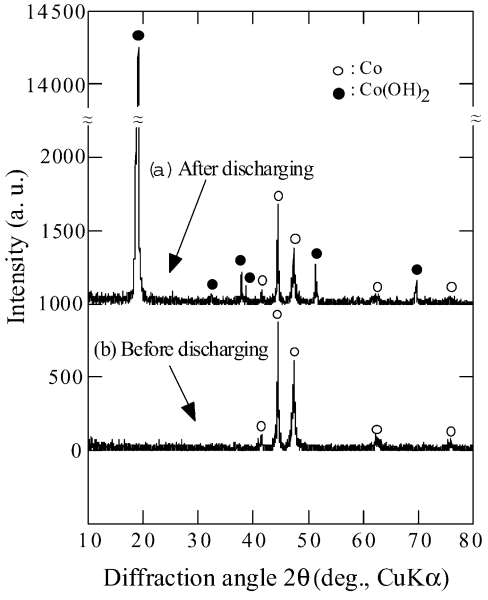

Fig. 5. XRD patterns of the anode electrode in the Co|KOH|O_2 cell (a) after 30 min discharging at 0.5 mA cm^{-2} and (b) before discharging.

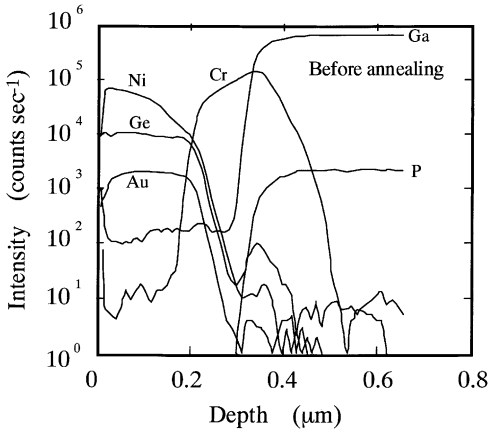

Fig. 6. SIMS depth profiling of the Au–Ge–Ni(/Cr)/GaP interface in the hybrid electrode before annealing.

displacement of Ga and Ge atoms. Ni realizes Ge diffusion easily by reducing the free energy of the GaP. Ge diffusion into the GaP increases the donor density at the interface. As a result, the energy barrier thickness is reduced, and the electrons can tunnel through this barrier. Cr reinforces the adhesion between the Au–Ge–Ni and GaP. As mentioned above, Au–Ge–Ni alloy reduces the energy barrier by means of the Ge diffusion in the GaP. To confirm the Ge diffusion, we measured the SIMS depth profiles of the Au–Ge–Ni(/Cr)/GaP interface. Fig. 6 shows SIMS depth profiles of the sample before annealing. Fig. 7 shows depth profiles of a sample that we annealed in a hydrogen atmosphere with an infrared lamp furnace at 600°C. These profiles indicate that the annealing resulted in the Ge being well-diffused in the GaP.

To confirm that the photoinduced electrons generated at the GaP/electrolyte interface actually reduced the oxidized Co, we studied the way in which electrochemical behavior is affected by combining Co and GaP in a Co–GaP hybrid electrode. Fig. 8 shows cyclic voltammograms that we measured with the GaP electrode under dark and illuminated conditions. In the dark (A), there was no obvious oxidation

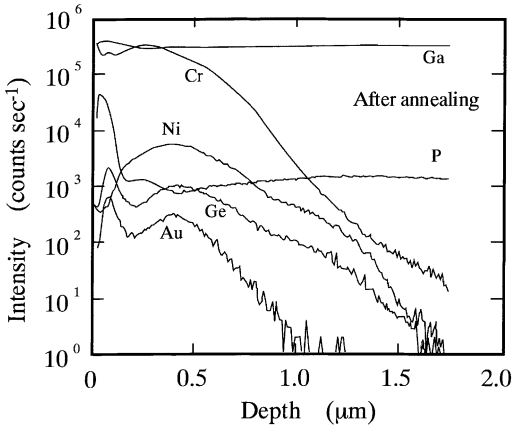

Fig. 7. SIMS depth profiling of the Au–Ge–Ni(/Cr)/GaP interface in the hybrid electrode, which was annealed in a hydrogen atmosphere with an infrared lamp furnace at 600°C.

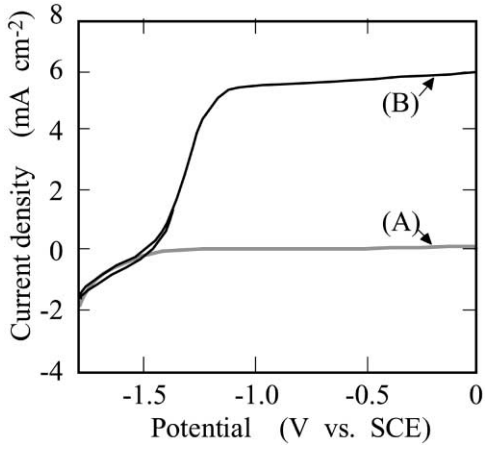

Fig. 8. Cyclic voltammograms at the GaP electrode in 2 M KOH: (A) in the dark; (B) when illuminated.

current. By contrast, under illuminated conditions (B), the photocurrents were observed at potentials positive of −1.4 V versus SCE, and saturates at about 6 mA cm^{-2}. This indicates that the flatband potential of the GaP electrode under this experimental condition is about −1.4 V versus SCE. Therefore, if the redox potential of the anode active material is more positive than −1.4 V, it is possible to reduce the anode active material with the photoinduced electrons. In this voltammogram, the appearance of photocurrents indicates the possibility of photo-induced oxygen evolution.

Cyclic voltammograms measured with the Co–GaP hybrid electrode under dark and illuminated conditions are shown in Fig. 9. The voltammogram measured in the dark (A) can be regarded as that of the Co electrode, because the voltammogram of the GaP electrode under the same conditions shows no clear reaction in the measured potential range as shown in Fig. 8. This voltammogram shows that the Co oxidation begins at −1.0 V versus SCE, which is more positive than the flatband potential of the GaP as mentioned above. Under illuminated conditions (B), we regard the shape of the voltammogram to be a combination of the voltammogram measured in the dark and the voltammogram

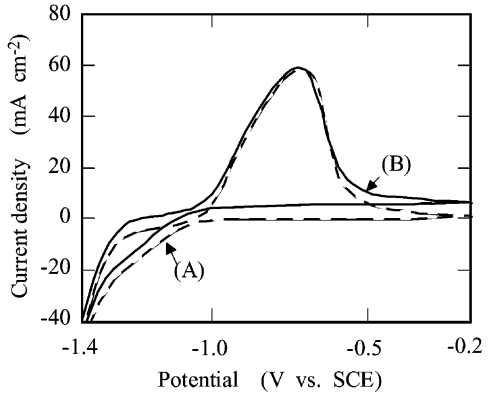

Fig. 9. Cyclic voltammograms at the Co–GaP hybrid electrode in 2 M KOH: (A) in the dark; (B) when illuminated.

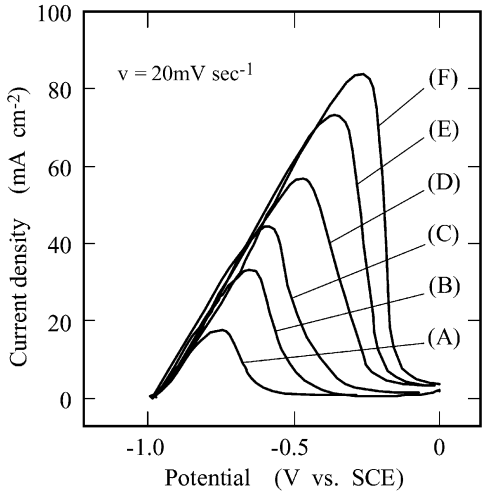

Fig. 10. Effect of illumination time on the voltammogram of the Co–GaP hybrid electrode: illumination times are (A) 1 min; (B) 2 min; (C) 3 min; (D) 5 min; (E) 10 min and (F) 20 min.

measured with the GaP electrode when illuminated. Cathodic currents due to reduction of the oxidized Co were observed at potentials negative of −1.1 V versus SCE, as recognized from the voltammogram shown in Fig. 9. Since the potential of −1.1 V is much more positive than the flatband potential of n-GaP, the photoinduced electrons in the band edge transfer can be utilized for reduction of the oxidized Co. Thus, we can see that the Co–GaP hybrid electrode functions as both an anode active and a photoabsorptive material.

To confirm that the photoinduced electrons is used to reduce the oxidized Co, we investigated the relationship between the illumination time and the Co anode peak at the Co–GaP hybrid electrode. After anodically oxidizing the hybrid electrode at −0.5 V versus SCE for about 60 min, we illuminated the GaP side of the electrode for various lengths of time, from 1 to 20 min, under open circuit conditions. After illumination, we scanned the electrode potential in the anodic direction from the rest potential under dark conditions. The results are shown in Figs. 10 and 11. In Fig. 11, i_p

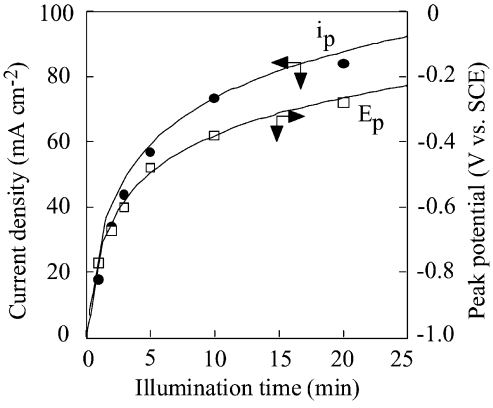

Fig. 11. Illumination time dependence of i_p and E_p, which show the anodic peak current and potential with the maximum current, respectively.

and E_p, which we obtained from the results shown in Fig. 10, show the anodic peak current and potential with the maximum current, respectively. Since the anodic peak corresponding to the Co oxidation increases with illumination time, the photocurrent generated at the GaP/electrolyte interface clearly reduces the oxidized Co attached to the back of the GaP. Furthermore, the illumination time dependence of the E_p indicated that the photo-reduction on this hybrid electrode progressed from the $Co(OH)_2$/Co layer interface towards the electrode top surface. This dependence is believed to be caused by the oxidation reaction of Co beneath the $Co(OH)_2$ layer. In such a limited space as the inside of a layer, OH^- diffusion into the Co through the $Co(OH)_2$ layer is disturbed and pH usually decreases. We consider the E_p potential shift to be caused by the decrease in the pH (OH^- deficiency).

Our electrochemical experiments with the Co–GaP hybrid electrode revealed that illumination of the GaP side causes reduction of the oxidized Co layer. This photo-reduction of the oxidized Co corresponds to the photo-charging reaction in the GaP–Co|KOH|O_2 cell. We, therefore, assembled a GaP–Co|KOH|O_2 cell consisting of the Co–GaP hybrid electrode and a Pt mesh electrode in order to study the photo-charging characteristics. The results obtained are shown in Fig. 12. During the first charge–discharge cycle, this cell was charged with a constant current of 1 mA for 1 h 20 min; the cell was then discharged with a constant current of 1 mA. During the second cycle, this cell was illuminated for 20 min in an open circuit condition; the cell then discharged in the dark at a constant current, as in the first cycle. During illumination, we observed the oxygen gas evolution on the GaP surface of the hybrid electrode. The cell voltage increased slightly during illumination, indicating the photo-reduction of the hybrid electrode. As a result, the cell was able to deliver a large capacity in the dark after illumination. The changes in cell voltage during discharging in both cycles have almost the same pattern. These results indicate that the cell is charged by illumination. During discharging, the Pt mesh electrode had a constant potential of 0.2 V versus SCE, which indicated reduction of oxygen. Furthermore, the discharge capacity of the cell, which removed oxygen (except dissolved one) by nitrogen gas filling, decreased to less than one-tenth of that of original one distinctly. The discharge performance of this cell recovered to that of original one by replacing nitrogen with air. These results indicate that the Pt mesh electrode works as the air electrode.

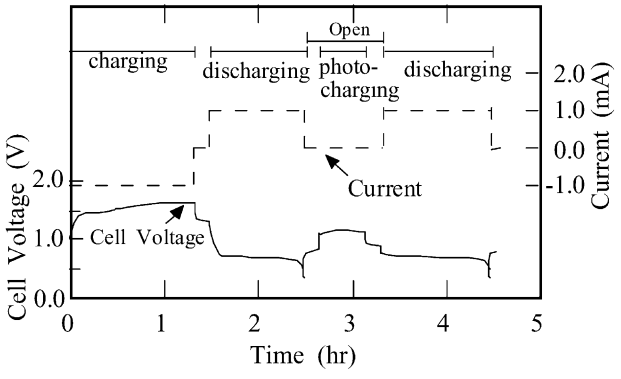

Fig. 12. Charge–discharge characteristics of GaP–Co|KOH|O_2 cell; the solid and dashed lines indicate the changes in cell voltage and current, respectively.

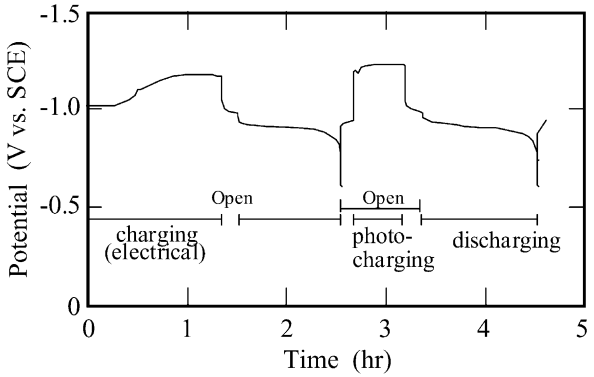

Fig. 13. Potential change in the Co–GaP hybrid electrode during charge–discharge cycles.

The cell voltage during electrical charging is much higher than that during light illumination, although much less photo-charging time is required to discharge the same amount of electricity than with electrical charging. This high voltage during electrical charging is caused by the overvoltage of the air electrode. The potential changes of the Co–GaP hybrid electrode with the same charge–discharge cycles as in Fig. 12 are shown in Fig. 13. The vertical axis is defined as the negative potential for easy comparison with Fig. 12. The electrode potential during illumination is more negative than during electrical charging. The higher charging rate with illumination shown in Fig. 12 is caused by the larger negative potential of the Co–GaP hybrid electrode. Because the cell voltage is determined by the difference between hybrid electrode and air electrode potentials, the high cell voltage found during electrical charging in Fig. 12 implies that the air electrode has a more positive potential, namely the air electrode has a large overvoltage when electrically charged.

The relation between the discharge capacity and the illumination time of the GaP–Co|KOH|O_2 cell is shown in Fig. 14. The open circles indicate the results obtained with a light source of the same intensity (100 mW cm^{-2}) as that used in the experiments described above. Discharge was carried out at a constant current of 1 mA. The photo-charging rate gradually decreased as the illumination time increased. To clarify the cause of this non-linearity between illumination time and discharge capacity, we obtained another set of data with the light source intensity reduced to one-fifth (20 mW cm^{-2}). The closed circles in the figure show the results. When the illumination time was less than 20 min, the discharge capacity increased in proportion to the

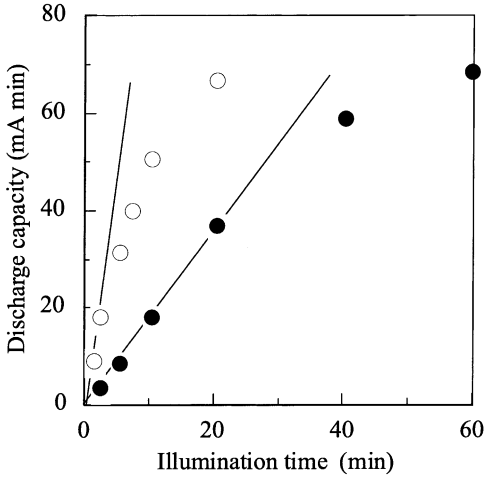

Fig. 14. Discharge capacity as a function of illumination time, the open circles show the results obtained with a light source that was the same as in the other experiments (100 mW cm^{-2}), the closed circles show the results obtained with a reduced-intensity light source (20 mW cm^{-2}).

illumination time. Fig. 15 shows the potential changes of the hybrid electrode during illumination with a lower light intensity. The electrode potential changed rapidly after about 20 min of illumination. We observed gas evolution on the Co surface at the same time. This suggests that the hydrogen evolution reaction starts to occur simultaneously after some degree of reduction, and that the consumption of the photoinduced electrons resulting from this hydrogen evolution reduces the charging efficiency.

Because the photo-charge reaction in this cell occurs only on the Co–GaP hybrid electrode, we were unable to measure the photo-charging current. Therefore, we estimated its value from the relationship between the discharge capacity and illumination time (Fig. 14). We calculated the photo-charging current during illumination with 100 and 20 mW cm^{-2} light sources as 9.3 and 1.9 mA from the slope of the plot in the early stages of photo-charging. These values are equivalent to 6.5 and 1.3 mW, since we estimate the average cell voltage during discharge to be 0.7 V from the discharge characteristics shown in Fig. 12. Both values

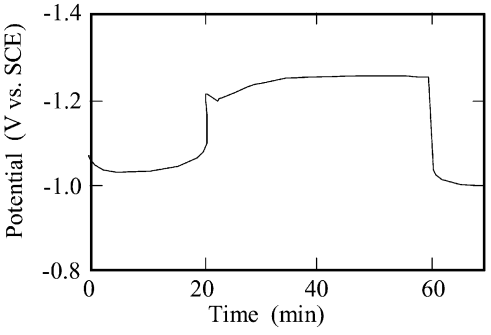

Fig. 15. Potential change at the Co–GaP hybrid electrode during illumination with a 20 mW cm^{-2} light source.

indicated that the photo-charge efficiency of this cell was about 3.0%.

The cell reaction, excluding the GaP dissolution reaction, seems to be as follows:

(1) Discharging

Negative electrode (Co–GaP):

$$Co + 2OH^- \rightarrow Co(OH)_2 + 2e^- \quad (2)$$

Positive electrode (oxygen catalyst):

$$\tfrac{1}{2}O_2 + H_2O + 2e^- \rightarrow 2OH^- \quad (3)$$

Overall reaction:

$$Co + \tfrac{1}{2}O_2 + H_2O \rightarrow Co(OH)_2 \quad (4)$$

(2) Photo-charging

Negative electrode (Co–GaP):

$$h\nu \rightarrow 2e^- + 2h^+ \quad (5)$$

$$Co(OH)_2 + 2e^- \rightarrow Co + 2OH^- \quad (6)$$

$$2OH^- + 2h^+ \rightarrow \tfrac{1}{2}O_2 + H_2O \quad (7)$$

Overall reaction:

$$Co(OH)_2 \rightarrow Co + \tfrac{1}{2}O_2 + H_2O \quad (8)$$

The charge–discharge characteristics can be explained in terms of the above photo-electrochemical reaction. That is, during photo-charging, light energy is stored in the negative electrode as the reduction product (Co) of oxidized cobalt ($Co(OH)_2$), and oxygen is created simultaneously. By contrast, during discharging, the Co reacts with oxygen and water. Electric energy is then generated by this reaction. On the long-term use of cell, the GaP surface of Co–GaP hybrid electrode becomes slightly rough after repeated photo-charging and discharging. This surface change indicates that some photoinduced holes are used not only for oxidation of the electrolyte but also for GaP dissolution. As mentioned above, the hybrid electrode seems to be stabilized by surface modification. From this point on, the hybrid electrode must be stabilized to improve the reliability of this cell. We aim at the development of a hybrid electrode, with even better levels of performance.

5. Conclusions

We fabricated a Co–GaP hybrid electrode and showed that illuminating the GaP surface of the electrode can reduce the oxidized Co layer. This means that the electrode performs as both a photo-electrode and an anode active material. By combining this hybrid electrode with an air electrode, we can assemble a GaP–Co|KOH|O_2 cell with only two electrodes. We confirmed that this cell was charged by illumination. In the early photo-charging process, 3.0% of the irradiated light energy was stored in the hybrid electrode. The stability of the semiconductor that constitutes

the hybrid electrode must be improved in order to increase cell reliability.

References

[1] R. Memming, J. Electrochem. Soc. 125 (1978) 117.
[2] S. Licht, R. Tenne, G. Hodes, G. Dagan, J. Cahen, D. Manassen, R. Triboulet, J. Rioux, C. Levy-Clement, Appl. Phys. Lett. 46 (1985) 608.
[3] B. O'Regan, M. Gratzel, Nature 353 (1991) 737.
[4] R.N. Pandey, K.S.C. Babu, D. Singh, O.N. Srivastava, Bull. Chem. Soc. Jpn. 65 (1992) 1072.
[5] S.C. Kondapaneni, D. Singh, O.N. Srivastava, J. Phys. Chem. 96 (1992) 8094.
[6] A. Ennaoui, S. Fiechter, H. Tributsch, M. Giersig, R. Vogel, H. Weller, J. Electrochem. Soc. 139 (1992) 2514.
[7] S. Kohtani, A. Kudo, T. Sakata, Chem. Phys. Lett. 206 (1993) 166.
[8] K. Xiao, E.R. Gonzalez, A. Avani, S. Srinivasan, A.J. Appleby, Electrochim. Acta 38 (1993) 459.
[9] Y. Yonezawa, M. Okai, M. Ishino, H. Hada, Bull. Chem. Soc. Jpn. 56 (1983) 2873.
[10] H.J. Gerritsen, W. Ruppel, P. Wurfel, J. Electrochem. Soc. 131 (1984) 2037.
[11] P.G.P. Ang, A.F. Sammells, Faraday Discuss. Chem. Soc. 70 (1980) 207.
[12] M. Kaneko, T. Okada, Electrochim. Acta 35 (1990) 291.
[13] H. Imamura, M. Futsuhara, S. Tsuchiya, J. Hydrogen Energy 15 (1990) 337.
[14] P. Bratin, M. Tomkiewicz, J. Electrochem. Soc. 129 (1982) 2469.
[15] T. Fujinami, M.A. Mehta, M. Shibatani, H. Kitagawa, Solid State Ionics 92 (1996) 165.
[16] D. Kaneko, S. Uegusa, J. Adv. Sci. 11 (1999) 103.
[17] T. Kubota, S. Uegusa, J. Adv. Sci. 11 (1999) 99.
[18] T. Ishii, S. Uegusa, J. Adv. Sci. 11 (1999) 101.
[19] T. Nomiyama, H. Kuriyaki, K. Hirakawa, Synth. Met. 71 (1995) 2237.
[20] M. Sharon, P. Veluchamy, C. Natarajan, D. Kumar, Electrochim. Acta 36 (1991) 1107.
[21] S.S. Dhumure, C.D. Lokhande, Solar Energy Mater. 29 (1993) 183.
[22] D. Linden (Ed.), Handbook of Batteries and Fuel Cells, Vol. 10(1), McGraw-Hill, New York, 1984.
[23] R. Memming, G. Schwandt, Electrochim. Acta 13 (1968) 1299.
[24] R.L. Meek, N.E. Schumaker, J. Electrochem. Soc. 119 (1972) 1148.
[25] K.W. Frese Jr., M.J. Madou, S.R. Morrison, J. Electrochem. Soc. 128 (1981) 1939.
[26] Y. Nakato, K. Abe, H. Tsubomura, Ber. Bunsenges. Phys. Chem. 80 (1976) 1002.
[27] Y. Nakato, H. Tsubomura, Electrochim. Acta 37 (1992) 897.
[28] S.R. Morrison, Electrochemistry at Semiconductor and Oxidized Metal Electrodes, Plenum Press, New York, 1984, pp. 183–186.
[29] A.J. de Bethune, N.A. Swendeman Loud, Standard Aqueous Electrode Potentials and Temperature Coefficients at 25°C, Clifford A, Hampel, 1964.
[30] M. Pourbaix, Atlas of Electrochemical Equilibria in Aqueous Solutions, Pergamon Press, Oxford, 1966, pp. 322–329.
[31] H. Kimi, S.H. Park, T.W. Lee, M.P. Park, Mater. Lett. 39 (1999) 33.